Influence of exciton localization on the quantum efficiency of GaN/(In,Ga)N multiple quantum wells grown by molecular-beam epitaxy

S. Dhar,[a] U. Jahn, O. Brandt, P. Waltereit,[b] and K. H. Ploog
Paul-Drude-Institut für Festkörperelektronik, Hausvogteiplatz 5-7, D-10117 Berlin, Germany

(Received 7 November 2001; accepted for publication 22 May 2002)

Using cathodoluminescence spectroscopy, we investigate the dependence of the transition energy and quantum efficiency of a GaN/(In,Ga)N multiple quantum-well structure on both the temperature and excitation density. A coupled rate-equation model is introduced to explain the experimental results. Polarization field screening has been incorporated in a realistic manner by solving these coupled rate equations self-consistently along with the Schrödinger and Poisson equations. Our study suggests that exciton localization increases the internal quantum efficiency significantly. © *2002 American Institute of Physics.* [DOI: 10.1063/1.1493237]

GaN/(In,Ga)N quantum wells (QWs) are being successfully used as the active region of blue and green light emitting diodes (LEDs) and injection lasers. In spite of this striking technological advance, the emission process is affected by several peculiarities of this materials system and is still under debate.

Due to the strong spontaneous polarization and the large piezoelectric coefficient in wurtzite group-III nitrides,[1,2] large electrostatic fields (~MV/cm) are present in QWs. These fields lead to a redshift of the transition energy and a prolonged radiative decay time.[3]

The miscibility gap between GaN and InN (Ref. 4) is expected to result in compositional fluctuations in (In,Ga)N,[5,6] creating local potential minima which in turn can give rise to the localization of excitons.[7–9] While the occurrence of compositional fluctuations is expected to depend on the growth conditions, and may thus not be universal, it should not be ruled out *a priori*. If present, exciton localization results in a redshift of the transition energy and a prolonged radiative decay time, much like electrostatic fields.

Changing an external parameter may also not be sufficient for distinguishing between these two mechanisms. For example, blueshift of the transition energy with an increase in excitation density may be related to the saturation of localized states,[9] but also to screening of the internal electrostatic fields.[10] An unequivocal distinction between these mechanisms is thus not straightforward, but requires specifically designed measurement and modeling strategies.

In previous work,[11] we addressed this issue by investigating the temperature dependence of the radiative lifetime of GaN/(In,Ga)N MQWs via time-resolved photoluminescence spectroscopy. In this letter, we use stationary cathodoluminescence (CL) spectroscopy to gain insight into this issue.

We have investigated a number of samples, but for the sake of consistency we will here focus on one sample which was also used in our previous study.[11] This sample is a 10-period MQW consisting of 9 nm thick GaN barriers and 6 nm thick $In_{0.16}Ga_{0.84}N$ wells grown by plasma-assisted molecular-beam epitaxy (MBE) on a 6*H*-SiC substrate with a 1 μm thick GaN buffer layer. Details of growth are given elsewhere.[11] The emission intensity of this sample at 5 K is comparable to state-of-the-art GaN/(In,Ga)N MQWs grown by metalorganic vapor phase epitaxy (MOVPE), but about one order of magnitude lower at 300 K. The CL investigation was performed in a Carl Zeiss DSM 962 scanning electron microscope equipped with an Oxford mono-CL2 and a He-cooling stage. A grating monochromator and a cooled photomultiplier were used in conjunction with conventional photon counting techniques to disperse and detect the CL signal, respectively. The generation rate G was controlled by changing the excitation area, keeping the acceleration voltage ($V_0 = 4$ kV) and beam current ($I_b = 0.3$ nA, measured by a Faraday cup) constant, and determined according to the method reported in Ref. 12.

Figure 1 shows the CL spectra of the sample under consideration for two different excitation densities at 5 and 235 K. A blueshift, a significant narrowing in linewidth, and a simultaneous decrease of CL efficiency with an increase of excitation density is seen at 5 K, whereas a slight increase in CL efficiency is observed at 235 K. Obviously, the situations at high and low temperature are quite different, and may be qualitatively interpreted as follows. At low temperatures, bound excitons dominate at low excitation density. With an increase of excitation density, localized states become saturated,[8,9] causing a blueshift, spectral narrowing, and a decrease of quantum efficiency since the excitons are now free to reach nonradiative centers (note that screening of electrostatic fields would result in an increase of the quantum efficiency). At sufficiently high temperatures, the localized states will no longer be occupied, and the spectra will be virtually independent of the excitation density. Saturation of the nonradiative channel will eventually result in an increase of quantum efficiency, as is observed experimentally.

For a quantitative understanding, we next develop a model that describes this situation. Free and bound exciton densities (n_f and n_b) for a certain generation rate G are governed by the coupled rate equations,

[a]Author to whom correspondence should be addressed; electronic mail: dhar@pdi-berlin.de
[b]Present address: Materials Department, University of California, Santa Barbara, CA 93106.

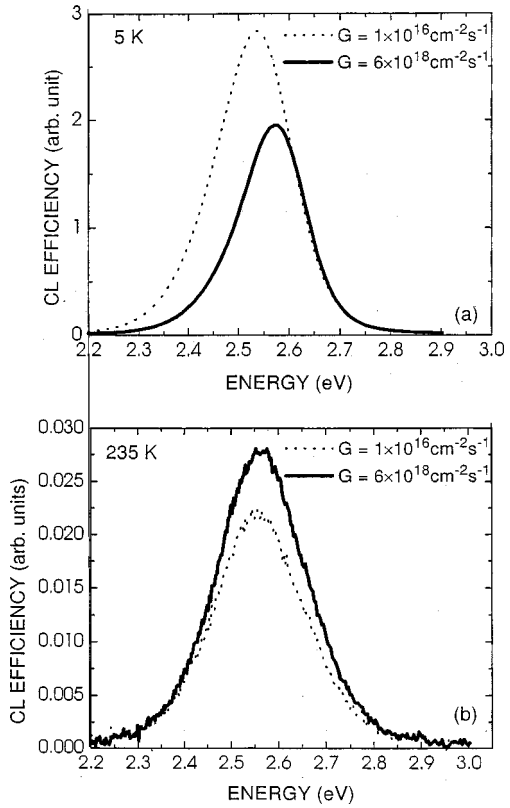

FIG. 1. Cathodoluminescence spectra at (a) 5 and (b) 235 K for two different generation rates. The generation rate is varied by changing the excitation area, and the spectra are thus a measure of the internal quantum efficiency.

$$G-\gamma_{\rm nr}n_f-\gamma_{rf}n_f+b_e n_b-b_r n_f(N_b-n_b)=0, \tag{1}$$

$$b_r n_f(N_b-n_b)-b_e n_b-\gamma_{rb}n_b=0, \tag{2}$$

where γ_{rf} and γ_{rb} are free and bound exciton radiative recombination rates, respectively, $\gamma_{\rm nr}$ is the nonradiative recombination rate of free excitons, b_e and b_r are emission and capture coefficients, respectively, and N_b is the density of localized states.

As done in our previous work and by other researchers,[13] we utilize a detailed balance to obtain

$$\sigma=\frac{b_r}{b_e}=\frac{1}{N_X}e^{E_b/k_BT}, \tag{3}$$

where σ is the cross section for capture of an exciton by a localized state, E_b is the localization binding energy, and N_X is the total density of extended states.

To get rid of the (principally unknown) emission and capture coefficients, we next assume the validity of the above detailed-balance criterion even under stationary conditions. While this assumption strictly holds true only at high temperatures, it can be shown to be an excellent approximation even at low temperatures due to the exponential nature of σ. We thus obtain a simple analytical solution to Eqs. (1) and (2) which depends only on the recombination rates and σ.

Next, we adopt the following conventions for the various recombination rates. The recombination rate of bound excitons, γ_{rb}, is assumed to be constant, as it should be for a zero-dimensional system. The nonradiative rate of free excitons, $\gamma_{\rm nr}$, is completely unknown, and is thus taken to be constant as a first (and crude) approximation (while nonradiative rates are known to strongly depend on the both temperature and excitation density, there is no way to *a priori* predict these dependencies). Finally, the radiative rate of free excitons may be expressed as $\gamma_{rf}=aR/T$, where a is a constant, $R=|\langle\psi_e|\psi_h\rangle|^2$ is the overlap integral, and the subscripts e and h stand for electron and hole, respectively. In principle, under stationary conditions only the ratio of these rates matters, but since we do have low temperature time-resolved measurements for this sample, we take γ_{rb} to be equal to the experimental value of 0.02 $\rm ns^{-1}$.

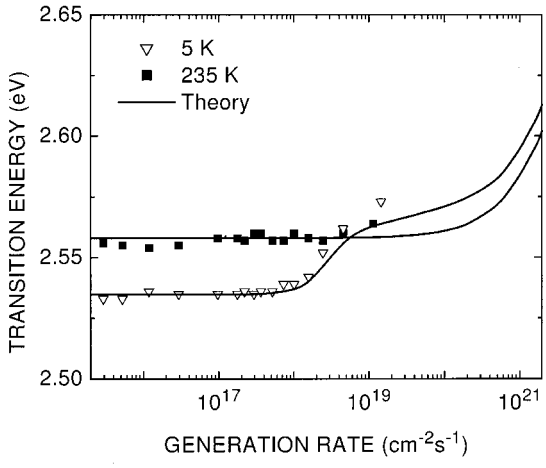

FIG. 2. Transition energy as a function of the generation rate at 5 (triangles) and 235 K (closed squares). The solid lines are the theoretical results.

The overlap integral is obtained by solving Eqs. (1) and (2) in conjunction with the Schrödinger and Poisson equations in a self-consistent manner (the polarization charges are taken from Ref. 1). To do this, we assume that the densities of excitons equal that of electrons and holes, which in turn are presumed to also be equal (in general, this is incorrect if impurities and deep centers are involved in the recombination process). However, in this way we easily obtain n_f, and once self-consistency is achieved, n_b can be obtained from Eqs. (1) and (2). Finally, the quantum efficiencies η_f and η_b for the free and bound excitons are defined as

$$\eta_f=\frac{\gamma_{rf}n_f}{G}, \tag{4}$$

$$\eta_b=\frac{\gamma_{rb}n_b}{G}, \tag{5}$$

and the total quantum efficiency will be $\eta=\eta_f+\eta_b$. The free parameters of our model are the constants N_b, E_b, a, and $\gamma_{\rm nr}$.

Figure 2 displays the experimental dependence of the transition energy on the excitation density as well as the best fit of our model to the data. The fits were obtained by the superposition of two Gaussians spectrally separated by 34 meV (E_b) whose intensity is given by $\gamma_{rf}n_f$ and $\gamma_{rb}n_b$. The model reproduces the general trend of the data well, confirming the qualitative interpretation given above. Screening of the polarization fields is predicted to occur at generation rates above 10^{20} $\rm cm^{-2}\,s^{-1}$, resulting in a strong blueshift at both low and high temperatures.

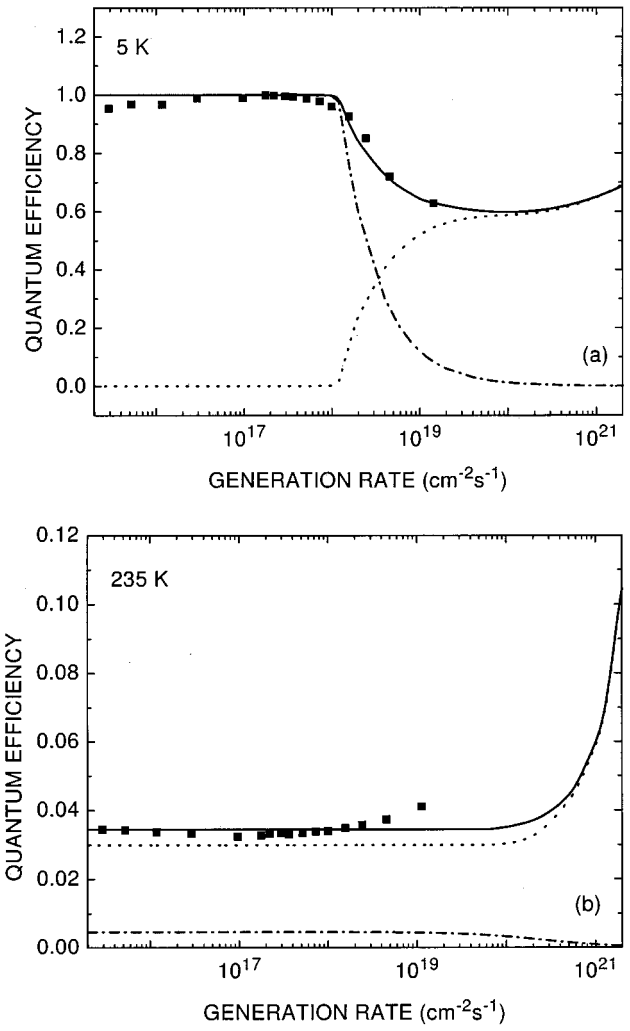

FIG. 3. Quantum efficiency (closed squares) as a function of the generation rate at (a) 5 and (b) 235 K. Theoretical results are shown by solid lines. Free and bound exciton contributions to the total quantum efficiency are shown by dotted and dash-dotted lines, respectively.

Figure 3 shows the experimental dependence of quantum efficiency on the excitation density at 5 [Fig. 3(a)] and 235 K [Fig. 3(b)] as well as the best fit of our above model to the data. This fit was done simultaneously with that of the experimental dependence of the quantum efficiency on the temperature at two different excitation densities, as shown in Fig. 4. As can be seen, the fits are quite satisfactory, in that they reproduce the general trends very well. The slight increase of the quantum efficiency in Fig. 3(b) is likely due to saturation of the nonradiative channel, which cannot be reproduced by our model because of our linearized treatment of the nonradiative rate.

The overall interpretation of these results is analogous to that given above, i.e., the changes with temperature and excitation density are due to exciton localization and nonradiative recombination. Screening of the internal fields is predicted to occur by our model, but at densities higher than those we can reach. Quantitatively, the fits shown in Figs. 2–4 give the following values for the fit parameters: a corresponds to $aR=14\ \mathrm{ns}^{-1}\,\mathrm{K}$ for low density of excitation, $N_b=5\times10^9\ \mathrm{cm}^{-2}$, $E_b=34\ \mathrm{meV}$, and $\gamma_{\mathrm{nr}}=2\ \mathrm{ns}^{-1}$. It is instructive to compare these values to those obtained in our previous work by experimentally different means for a different sample.[11] The values for N_b and E_b are identical within the uncertainty. In fact, E_b is close to the calculated change in transition energy (31 meV) for a well-width fluctuation of ±1 monolayer. It is thus conceivable that localization in these samples occurs at well-width fluctuations and hence has a well-defined depth.

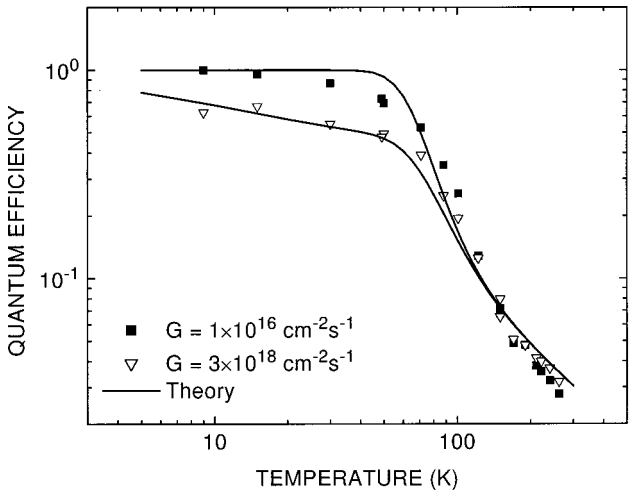

FIG. 4. Variation of the quantum efficiency with the temperature for two different generation rates. Theoretical results are shown by solid lines.

[1] F. Bernardini, V. Fiorentini, and D. Vanderbilt, Phys. Rev. B **56**, R10024 (1997).
[2] K. Shimada, T. Sota, and K. Suzuki, J. Appl. Phys. **84**, 4951 (1998).
[3] P. Waltereit, O. Brandt, A. Trampert, H. T. Grahn, J. Menniger, M. Ramsteiner, M. Reiche, and K. H. Ploog, Nature (London) **406**, 865 (2000).
[4] I. Ho and G. B. Stringfellow, Appl. Phys. Lett. **69**, 2701 (1996).
[5] D. Doppalapudi, S. N. Basu, K. F. Ludwig, and T. D. Moustakas, J. Appl. Phys. **84**, 1389 (1998).
[6] M. K. Behbehani, E. L. Piner, S. X. Liu, N. A. El-Masry, and S. M. Bedair, Appl. Phys. Lett. **75**, 2202 (1999).
[7] S. Chichibu, T. Azuhata, T. Sota, and S. Nakamura, Appl. Phys. Lett. **69**, 4188 (1996).
[8] P. G. Eliseev, P. Perlin, J. Lee, and M. Osiński, Appl. Phys. Lett. **71**, 569 (1997).
[9] M. Osiński, P. Perlin, P. G. Eliseev, J. Lee, and V. A. Smagley, J. Cryst. Growth **189/190**, 803 (1998).
[10] F. D. Sala, A. Di Carlo, P. Lugli, F. Bernardini, V. Fiorentini, R. Scholz, and J. M. Janku, Appl. Phys. Lett. **74**, 2002 (1999).
[11] P. Waltereit, O. Brandt, J. Ringling, and K. H. Ploog, Phys. Rev. B **64**, 245305 (2001).
[12] The number of generated electron-hole pairs per second can be expressed [see, e.g., C. J. Wu and D. B. Wittry, J. Appl. Phys. **49**, 2827 (1978)] as $G_0=6.25\times10^{21}V_0I_b(1-\eta\bar{V}/V_0)/\epsilon$, where $\epsilon\simeq10$ eV is the mean energy required to generate an electron-hole pair in eV, $\eta\simeq0.2$ is the fraction of backscattered electrons, and $\bar{V}\simeq0.65V_0$ is the mean energy of the backscattered electrons in kV. The generation rate G of carriers per unit area in a single quantum well is obtained by dividing G_0 by 5 [Monte Carlo simulations, using the commercial program MC-SET developed by E. Napchan (DLM Enterprises), show that for the present beam energy, the carriers are mostly generated within the first five QWs] and by the area of the electron beam spot. The spot area is varied between 0.8 and 5000 μm^2 by defocusing the electron beam in adjustable steps and is measured by exposing a resist layer like what is used for electron beam lithography.
[13] See, for example, O. Brandt, J. Ringling, K. H. Ploog, H.-J. Wünsche, and F. Henneberger, Phys. Rev. B **58**, R15977 (1998), and references therein.